MR Elastography of the Liver in an Animal Model of Hepatic Fibrosis

M. Yin[1], A. Manduca[1], P. C. Harris[2], V. E. Torres[2], R. L. Ehman[1]

[1]Department of Radiology, Mayo Clinic College of Medicine, Rochester, MN, United States, [2]Department of Nephrology and Hypertension, Mayo Clinic College of Medicine, Rochester, MN, United States

Introduction At present, the gold standard for diagnosing hepatic fibrosis is liver biopsy, which is an invasive procedure, with risks of complications, potential sampling errors, and known problems with subjective histology grading. MR Elastography (MRE)(1) is a modified phase-contrast MRI technique for quantitatively assessing the mechanical properties of soft tissues by visualizing propagating shear waves. Several studies have shown that fibrosis is associated with increased liver stiffness (2, 3), which also agrees with the clinical experience of manual palpation in the diagnosis of cirrhosis. Thus, MRE could be a promising non-invasive diagnostic method to overcome the aforementioned limitations and become a sensitive quantitative indicator of hepatic fibrosis. However, the underlying relationship between hepatic fibrosis extent and the corresponding mechanical properties of the liver tissues has not been quantitatively evaluated yet in an in vivo animal model. Therefore, this research had three specific aims: 1. to obtain high quality wave images in an animal model of hepatic fibrosis (ARPKD = autosomal recessive polycystic kidney disease in mice) by optimizing MRE imaging protocols using a specialized driver system; 2. to obtain reliable mean shear stiffness by implementing a phase gradient inversion algorithm (4); 3. to evaluate the relationship between the estimated shear stiffness and fibrosis stage in this detailed animal model.

Materials and Methods All experiments were implemented on a 1.5 T whole-body GE imager (Signa, GE Medical System, Milwaukee, WI), using a 3-inch surface coil. Gradient Echo MRE imaging with continuous shear wave drive was used to shorten the TR time. A 0.4×39mm silver needle applicator (5) was mounted on an electromechanical driver with longitudinally-orientated vibrations as shown in Fig.1. This specific longitudinal driver with internal excitation was then tested in a homogeneous 15% B-gel phantom to investigate the generated shear wave field for optimizing the imaging protocols. The phase gradient inversion algorithm was also evaluated for accuracy and efficiency on the acquired wave images.

The MRE imaging protocols were first tested in 15-week normal rats to evaluate feasibility and then applied to the even smaller ARPKD and control mice aged from 3 to 12 months old respectively. The animals were anesthetized with ketamine 50 mg/Kg and xylazine 5 mg/Kg IP. After shaving and preparation of the abdomen, they were placed under the surface coil in a supine position. The needle driver was inserted in liver tissues from the anterior as shown in the top two figures of Fig.2. The imaging parameters of the selected optimum coronal planes were: FOV = 10 cm; TR/TE: 33.3/16 ms; resolution matrix: 256×64; driving frequencies: 90/120/150Hz; flip angle: 30°; 8 phase offsets. After acquiring MRE data, all the phase difference images were analyzed using a phase gradient inversion algorithm to estimate the mean shear stiffness of the hepatic tissues. The measurements were then evaluated using statistical tests and cross-sectional correlative analysis.

Fig. 1

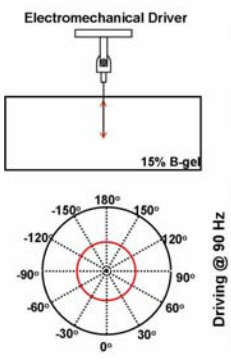

Fig. 2

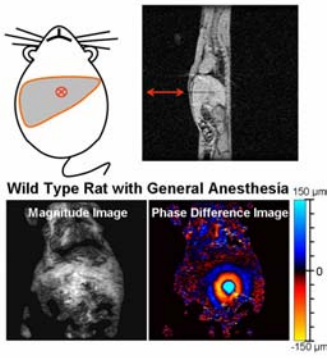

Results The phantom study with the needle driver demonstrated that the performance of the generated shear wave field was identical to the theoretical result as shown in the bottom polar plot of Fig.1. The coronal imaging planes perpendicular to the needle driver were verified to be optimum for both shear wave visualization and shear stiffness estimation as shown in the bottom two MRE images of Fig.2. The shear wave fronts appeared as circles, as shown in the wave images, radiating from the location of the vibrating needle through the imaging plane. The optimized MRE imaging protocols were then applied to ARPKD mice and their control groups. The phase gradient inversion algorithm was implemented to calculate the wave number ($k = 2\pi/\lambda$) of the propagating shear waves by taking multiple 1-D profiles in the 1st harmonic phase gradient image as shown in the upper two images of Fig. 3, 4. All 1-D phase profiles were radiating from the vibrating source to the liver edges. The mean shear stiffness ($\mu = 4\pi^2f^2/k^2$) was then evaluated from the slope of a straight line fit to the unwrapped phase gradient profiles (Fig. 3, 4 bottom plots). Average shear stiffness measurements were taken at all three different driving frequencies.

Fig. 3

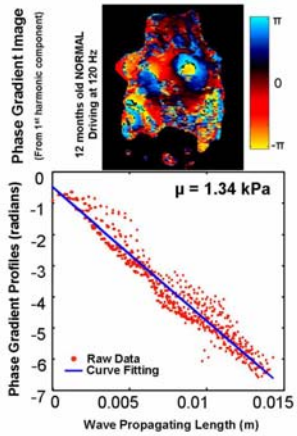

Fig. 4

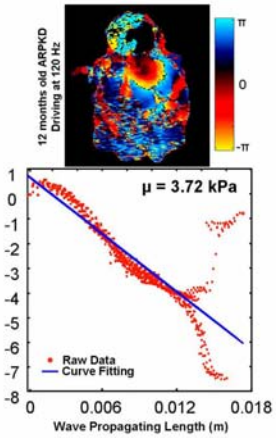

Fig. 5

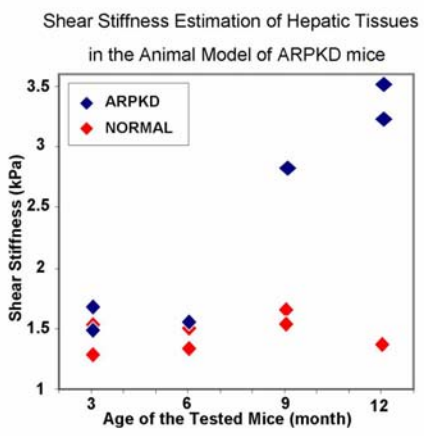

As shown in Fig. 5, the wild type control mice (7, average weight = 37.7 ± 9.2 g) have a mean liver shear stiffness of 1.45 ± 0.13 kPa; there is no significant difference between any two age groups. The ARPKD mice (6, average weight = 30.6 ± 9.9 g) have a mean liver shear stiffness of 2.37 ± 0.91 kPa. The elder ARPKD groups (9~12 months old) have a significantly higher stiffness than the younger ARPKD groups (3~6 months old) ($p < 0.05$). A significant difference was also evident in the measured shear stiffness of all the ARPKD mice and their control mice ($p < 0.05$).

Discussion For genetic knockout ARPKD mice, diffuse hepatic fibrosis and cysts develop progressively with age. Therefore, this preliminary study allows us to closely follow the relationship between the shear stiffness of liver tissues and extent of hepatic fibrosis, as measured by histology. These preliminary results demonstrate that the shear stiffness of the liver tissue increases systematically with the extent of hepatic fibrosis in the ARPKD animal model. We expect that the completed study, which will include measurements of over 30 animals, will define the relationship more precisely.

Conclusion MR Elastography is an effective quantitative method to assess the in vivo mechanical properties of the liver tissues in small animals, allowing the relationship between histologic fibrosis and mechanical properties of liver tissues to be defined.

Reference [1] R. Muthupillai, Science 1995, 269: 1789-1936. [2] WC Yeh, Ultrasound Med Biol 2002, 28: 467-474. [3] O Rouviere, Radiology, in press [4] A. Manduca, Med Image Anal 5(4): 237-254, 2001. [5] Q.C.C. Chan, ISMRM 2005, 2010.